

Layer-resolved conductivities in multilayer graphenes

Takeo Wakutsu,¹ Masaaki Nakamura,¹ and Balázs Dóra²

¹*Department of Physics, Tokyo Institute of Technology,
Oh-Okayama, Meguro-ku, Tokyo 152-8551, Japan*

²*Department of Physics, Budapest University of Technology and Economics, Budafoki út 8, 1111 Budapest, Hungary*

We study interlayer transport of multilayer graphenes in magnetic field with various stacking structures (AB, ABC, and AA types) by calculating the Hall and longitudinal conductivities as functions of Fermi energy. Their behavior depends strongly on the stacking structures and selection of the layers. The Hall conductivity between different layers is no longer quantized. Moreover, for AB stacking, the interlayer conductivity vanishes around zero energy with increasing layer separation, and shows negative values in particular cases. The fact that longitudinal interlayer conductivity suppressed by the magnetic field indicates that this system can be applied as a switching device.

PACS numbers: 72.80.Vp,73.22.Pr,81.05.ue,71.70.Di

—*Introduction*— Graphene has attracted increasing attention since its first isolation from graphite in 2004 [1]. Graphene consists of two-dimensional hexagonal lattice of carbon atoms, whose quasiparticles are governed by a massless Dirac equation. A variety of unusual phenomena are observed in this system such as universal value of the minimum conductivity, anomalous quantum Hall effect, and so on [2–4]. In addition, bilayer graphene has also been studied intensely [5–8], which is characterized by intrinsic Landau level degeneracy at zero energy and a gate tunable band gap.

Due to the qualitative differences between mono- and bilayer graphene, a lot of interest has been focused on multilayer graphenes to determine, how additional layers influence their physical response. One of the most intriguing property of these systems is the variety of stacking structures such as AB (Bernal), ABC (rhombohedral) and AA (simple hexagonal) types. Graphene is usually produced by micro-mechanical cleavage of graphite, so that the stacking structure is usually of AB type, since the natural graphite falls into this category. However, production of graphene with other stacking types is also possible by recent technology such as epitaxial methods [9, 10]. In addition, AA stacking can be realized by folding of a graphene sheet [11]. In terms of band structure, multilayer graphenes with more than 10 layers are regarded as bulk graphite [12], so that few layer graphenes have been considered to be important systems, interpolating between graphene and graphite. So far, diamagnetism [13], transport properties [14–21], and energy spectra [22, 23] have been studied for these systems.

In this Letter, we investigate the transport properties between two different layers of multilayer graphenes in magnetic field as illustrated in Fig. 1, using the Kubo formula. Here, while electric current is run through a given layer, the resulting voltage drop or induced current is measured in another layer. In order to calculate these “layer-resolved conductivities”, we establish the formalisms to obtain eigenvalues and eigenstates of multilayer systems, using the block diagonalization tech-

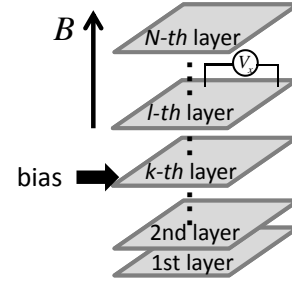


FIG. 1: Schematic illustration of the layer-resolved magneto transport between k -th and l -th layers in a multilayer graphene.

nique. We find many interesting properties such as negative response and switching effect by magnetic field, absent in monolayer graphene.

—*Formalism*— We consider three types of the stacking structures of multilayer graphenes, AB, ABC and AA types. Since a monolayer graphene consists of two sublattices labeled by A and B, carbon atoms in multilayer graphenes are specified by (A_i, B_i) meaning the A, B sublattices in the i -th layer, respectively. Figure 2 shows the lattice structure of these systems with nearest neighbor intralayer (interlayer) coupling t (t_\perp).

Among these three types, we discuss AB stacked graphene in detail which is the most common structure of graphite. After taking the continuum limit of tight-binding model, in a basis with atomic components for N layers, $|A_1\rangle, |B_1\rangle, \dots, |A_N\rangle, |B_N\rangle$, the model Hamiltonian in the vicinity of K point (per spin and per valley) is

$$\mathcal{H} = \begin{bmatrix} H_0 & V & 0 & 0 & 0 \\ V^\dagger & H_0 & V^\dagger & 0 & 0 \\ 0 & V & H_0 & V & 0 \\ 0 & 0 & V^\dagger & H_0 & \ddots \\ 0 & 0 & 0 & \ddots & \ddots \end{bmatrix}, \quad (1)$$

with

$$H_0 = \begin{bmatrix} 0 & v\pi_- \\ v\pi_+ & 0 \end{bmatrix}, \quad V = \begin{bmatrix} 0 & 0 \\ t_\perp & 0 \end{bmatrix}, \quad (2)$$

where $\pi_\pm \equiv \pi_x \pm i\pi_y$ with $\boldsymbol{\pi} \equiv \mathbf{p} + e\mathbf{A}/c$ being the momentum operator in a magnetic field $\nabla \times \mathbf{A} = (0, 0, B)$. $v = (\sqrt{3}/2)\alpha t/\hbar$ is the Fermi velocity with α being the lattice constant. We have ignored long-range hopping terms except for t and t_\perp for simplicity. Since the commutation relation between the momentum operators in Eq. (2) is $[\pi_\pm, \pi_\mp] = \mp 2eB\hbar/c$, there are correspondences with the creation and annihilation operators of the harmonic oscillator: $\pi_\pm \rightarrow \sqrt{2\hbar}a^\dagger$ and $\pi_\mp \rightarrow \sqrt{2\hbar}a$ for $eB \geq 0$, where $l \equiv \sqrt{c\hbar/|eB|}$.

In order to solve this model, we employ the matrix decompositions of the Hamiltonian. It is already known that the Hamiltonians of AB and AA-stacked N -layer graphenes can be block diagonalized, considering Fourier modes of the wave function along the stacking direction [13, 18, 21]. The same conclusion can also be obtained by factorization of determinant of the Hamiltonians [14]. According to these, the effective Hamiltonian of AB-stacked N -layer graphenes can be divided into isolated $[N/2]_G$ effective bilayer systems ($[x]_G$ is the integer part of x), and one monolayer system is added when N is odd. Similarly, the effective Hamiltonian of an AA-stacked N -layer graphene consists of N isolated monolayer systems with different potential energies.

Therefore, we can introduce a transformation matrix U for the AB stacked system which relates the wave function in the real space $|A_1\rangle, |B_1\rangle, \dots, |A_N\rangle, |B_N\rangle$ and that in the Fourier modes of stacking direction $|\phi_{N-1}^{(A, \text{even})}\rangle, |\phi_{N-1}^{(B, \text{even})}\rangle, |\phi_{N-1}^{(A, \text{odd})}\rangle, |\phi_{N-1}^{(B, \text{odd})}\rangle, |\phi_{N-3}^{(A, \text{even})}\rangle, \dots, |\Psi_\alpha\rangle, |\Psi_\beta\rangle$. Here we have used the notation defined in Refs. 13 and 23. Then the Hamiltonian \mathcal{H} is transformed into a block diagonalized form,

$$\mathcal{H}' = U^\dagger \mathcal{H} U = \begin{bmatrix} \mathcal{H}^{\text{sub}}(N-1) & & & \\ & \mathcal{H}^{\text{sub}}(N-3) & & \\ & & \ddots & \\ & & & \ddots \end{bmatrix}. \quad (3)$$

Here, $\mathcal{H}^{\text{sub}}(m)$ is a Hamiltonian of a bilayer system with an effective hopping

$$\mathcal{H}^{\text{sub}}(m) = \begin{bmatrix} 0 & v\pi_- & 0 & t_\perp \lambda_m \\ v\pi_+ & 0 & 0 & 0 \\ 0 & 0 & 0 & v\pi_- \\ t_\perp \lambda_m & 0 & v\pi_+ & 0 \end{bmatrix}, \quad (4)$$

with

$$\lambda_m = 2 \sin\left(\frac{m\pi}{2(N+1)}\right), \quad m = N-1, N-3, \dots > 0.$$

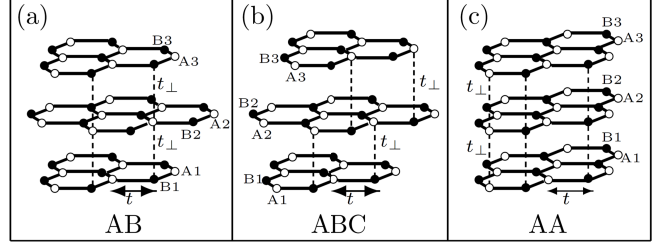


FIG. 2: Lattice structures of (a)AB, (b)ABC and (c)AA-stacked trilayer graphenes, containing six sites in a unit cell. White and black circles denote carbon atoms which belong to A and B sublattices in each layer.

Using the above block diagonalized Hamiltonian, we easily obtain eigenvalues of AB-stacked graphenes based on the known results for monolayer and bilayer systems, replacing the interlayer hopping t_\perp by the effective one $t_\perp \lambda_m$,

$$E_{m,n}^\mu = s_2 \frac{\sqrt{2}\hbar v}{l} \left\{ \frac{1}{2} \left(2n+1 + (\lambda_m r)^2 \right. \right. \\ \left. \left. + s_1 \sqrt{(\lambda_m r)^4 + 2(2n+1)(\lambda_m r)^2 + 1} \right) \right\}^{\frac{1}{2}}, \quad (5)$$

where $r \equiv \frac{l}{\sqrt{2}\hbar v} t_\perp$ and n denotes the Landau levels. The label $\mu \equiv (s_1, s_2)$ specifies the outer and the inner bands ($s_1 = \pm 1$), and positive and negative ($s_2 = \pm 1$) energies, respectively. The eigenstates of AB-stacked graphenes in basis of the real space $|A_1\rangle, |B_1\rangle, \dots, |A_N\rangle, |B_N\rangle$ are obtained from those of the subsystems $\mathcal{H}^{\text{sub}}(m)$ and the transformation matrices U , written as

$$|\Psi_{n,\mu}\rangle = \left[f_{n,\mu}^1 |n-1\rangle \quad f_{n,\mu}^2 |n\rangle \quad f_{n,\mu}^3 |n\rangle \quad f_{n,\mu}^4 |n+1\rangle \quad \dots \right]^T, \quad (6)$$

where $f_{n,\mu}^{2k-1}, f_{n,\mu}^{2k}$ denote coefficients of the wave function for the k -th layer, $|n\rangle$ is the number state of a, a^\dagger , and $1 \leq \mu \leq 2N$ is band indices of the multilayer system.

The conductivity is given by the Kubo formula as

$$\text{Re } \sigma_{ij}(\Omega) = -\frac{\text{Im } \Pi_{ij}(\Omega)}{\hbar\Omega}, \quad (7)$$

where Π_{ij} with $\{i, j\} \in \{x, y\}$ and Π_{ij} is the Fourier transform of the current-current correlation function obtained after analytic continuation of the Matsubara form. The general expression of the conductivity of the multilayer graphenes is obtained by extending the result for the bilayer graphene [7] as

$$\text{sgn}(eB)\sigma_{xy}(\Omega) + i\sigma_{xx}(\Omega) = -\frac{4e^2 v^2}{\hbar l^2 \Omega} \sum_n \sum_{\mu, \nu} \quad (8)$$

$$\left\{ X(E_{n+1}^\mu, E_n^\nu; \Omega) - X(E_{n+1}^\mu, E_n^\nu; -\Omega) \right\} \left(\sum_{k=1}^N f_{n+1,\mu}^{2k-1} f_{n,\nu}^{2k} \right)^2,$$

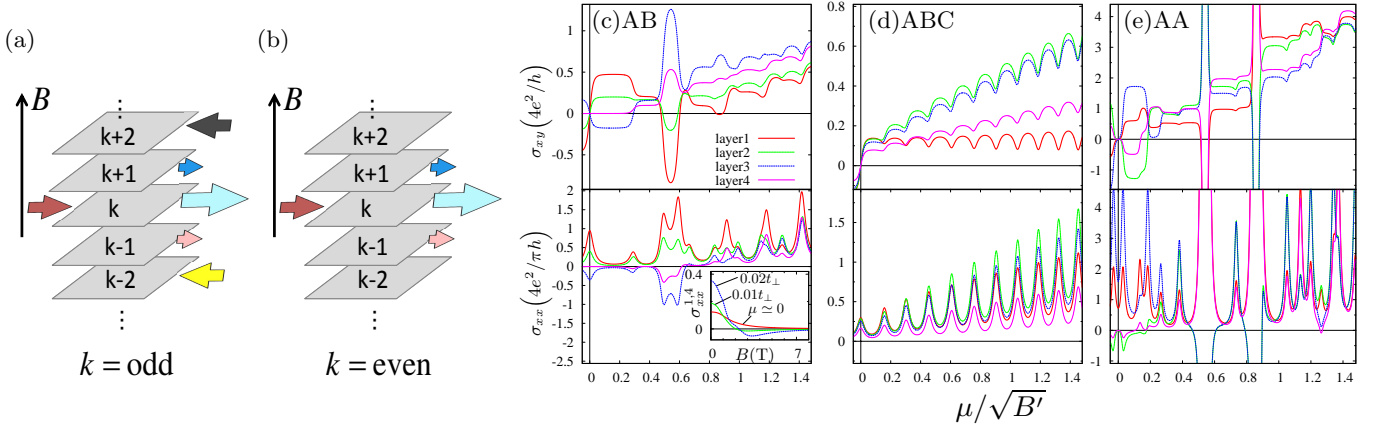


FIG. 3: Schematic illustration of intensity of the layer-resolved conductivity for AB-stacked multilayer graphene applying bias to the k -th layer where k is (a) odd and (b) even layers counting along the direction of the magnetic field. The layer-resolved Hall (σ_{xy}^{kl}) and longitudinal (σ_{xx}^{kl}) conductivities of 4-layer graphene in magnetic fields ($B = 14\text{T}$) for (c)AB, (d)ABC and (e)AA stacking. The bias is applied to the 1st layer. An inset in (c) shows σ_{xx}^{14} as functions of the magnetic field.

with

$$X(A, B; \Omega) \equiv \sum_n [(\tilde{i}\omega_n - A/\hbar)^{-1}(\tilde{i}\omega_{n+m} - B/\hbar)^{-1}]_{\nu_m \rightarrow \Omega} - (\Omega \rightarrow -\Omega)(\Omega\beta\hbar)^{-1}, \quad (9)$$

where $\tilde{\omega}_n$ is Matsubara frequency of fermion including the chemical potential and effect of impurity scattering Γ as $\tilde{i}\omega_n + [\mu + 1 \text{sgn}(\omega_n)\Gamma]/\hbar$. ν_m is the bosonic Matsubara frequency and $\omega_{n+m} \equiv \omega_n + \nu_m$.

In the above formalism, the electric current operators are defined by $J_i = -\frac{\delta \mathcal{H}}{\delta A_i}$ with A_i the vector potential in the direction $i = x, y$. Now, we introduce current operators for particular layers to calculate the conductivity between two distinct layers as $J_i^k = -\frac{\delta \mathcal{H}}{\delta A_i^k}$ where k denotes layer number ($k = 1, 2, \dots, N$), and A_i^k is the vector potential acting solely in layer k in direction i . The current operator of the k -th layer has only two matrix elements, $(J_i^k)_{2k-1, 2k}$ and $(J_i^k)_{2k, 2k-1}$, and all other elements are vanishing. The general expression for the layer-resolved conductivity between the k -th and l -th layers, σ_{ij}^{kl} is given by Eq. (8) with the following replacement,

$$\left(\sum_{k=1}^N f_{n+1, \mu}^{2k-1} f_{n, \nu}^{2k} \right)^2 \rightarrow f_{n+1, \mu}^{2k-1} f_{n, \nu}^{2k} f_{n+1, \mu}^{2l-1} f_{n, \nu}^{2l}. \quad (10)$$

In the present model which includes only the nearest interlayer couplings as interlayer matrix elements, the layer current operator, J_i^k does not have any momentum dependence. However, this situation can change if we introduce other matrix elements, such as tilted interlayer hoppings. In such cases, the layer current operators should be redefined appropriately so that they become Hermitian and satisfy the relation $J_i = \sum_{k=1}^N J_i^k$.

—Numerical results— Based on the above discussions, we calculate the layer resolved Hall conductivity σ_{xy}^{kl} of AB-stacked multilayer graphenes, as functions of the

Fermi energy, for strong magnetic field $\hbar\omega_c \gg \Gamma$ where $\omega_c \propto \sqrt{B}$ is the cyclotron frequency. Our findings are summarized as: i) σ_{xy}^{kl} is no longer quantized as integer times e^2/h . ii) around the zero energy $\mu \sim 0$, σ_{xy}^{kl} becomes almost zero when the source and the drain are separated by more than three layers $|k-l| \geq 3$ and the biased layer k is odd, and two layers $|k-l| \geq 2$ and k is even. iii) the layer resolved Hall response can be negative ($\sigma_{xy}^{kl} < 0$) around the zero energy for $|k-l| = 2$ when the biased layer k is odd. Layers indices are growing in the direction of the magnetic field. These features are summarized in Fig. 3(a),(b). Similar behavior can also be seen in the longitudinal conductivity σ_{xx}^{kl} which behaves like derivatives of σ_{xy}^{kl} by μ .

In Fig. 3 we show numerical results of σ_{xy}^{kl} for $N = 4$ as functions of the Fermi energy μ , where the bias is applied to the first layer, and $B' \equiv 2v^2 eB/c$. We have assumed $B = 14\text{T}$, $T = 0\text{K}$, $\Gamma = 0.01t_{\perp}$, $t = 3.16\text{eV}$, $t_{\perp} = 0.39\text{eV}$, and taken DC limit $\Omega \rightarrow 0$. We can see the above three features for AB staking in Fig. 3(c). Further, σ_{xx}^{14} is finite without magnetic field, meaning that property ii) is broken when magnetic field is turned off, as shown in the inset of Fig. 3(c). The conductivity vanishes when $B' \sim \Gamma$.

We also calculate layer resolved conductivities for other stacking structures. For ABC stacking, although the matrix decomposition technique is no longer available, we can diagonalize the Hamiltonian numerically to obtain the layer resolved conductivities. In this case, as shown in Fig. 3(d), the electric currents are induced in every layer. Moreover, the conductivities for ABC-stacking do not exhibit negative values even in the vicinity of zero energy.

For AA stacking, the matrix decomposition technique similar to AB stacking can also be used [18, 21]. We calculate the conductivities by setting the value of interlayer hopping as $t_{\perp}^{\text{AA}} = t_{\perp}^{\text{AB,ABC}}/2$. In this system, negative

conductivity also appears as shown in Fig. 3(e). In this case, it is difficult to summarize the features of layer-resolved conductivities in terms of simple rules, because the effective Hamiltonian consists of N monolayer systems with different Fermi energies, so that the number of Landau levels near the zero energy depends strongly on the strength of the magnetic field. In contrast to this, the Landau level structure is an intrinsic property for AB and ABC-stacked systems.

—*Analytical results for AB stacking*— In order to understand the above results for AB stacking in more detail, we calculate the first quantum Hall step of σ_{xy}^{kl} analytically for $\Gamma = 0$. We consider the following four cases: (a/b) $(k, l) = (\text{odd}, \text{odd})$ for $N = \text{even/odd}$, respectively, (c) $(k, l) = (\text{odd}, \text{even})$, (d) $(k, l) = (\text{even}, \text{even})$. Since layer indexes grow in the direction of the field, such classification is unique. We obtain the following results, defining $\tilde{\sigma}_{xy}^{k,l} \equiv \text{sgn}(eB) \frac{\hbar}{4e^2} \sigma_{xy}^{k,l}$,

$$\tilde{\sigma}_{xy}^{k,l(a)} = \left[\frac{r^2}{4} (\delta_{l',k'+1} - \delta_{k',1} \delta_{l',1}) + \frac{1+r^2}{2} \delta_{k',l'} \right] \times \sum_m \frac{U_{4k'-2,m} U_{4l'-2,m}}{1 + (\lambda_m r)^2} \quad (11a)$$

$$\tilde{\sigma}_{xy}^{k,l(b)} = \left[\frac{r^2}{4} (\delta_{l',k'+1} - \delta_{k',1} \delta_{l',1} - \delta_{k',\frac{N+1}{2}} \delta_{l',\frac{N+1}{2}}) + \frac{1+r^2}{2} \delta_{k',l'} \right] \times \left[\sum_m \frac{U_{4k'-2,m} U_{4l'-2,m}}{1 + (\lambda_m r)^2} + \frac{2(-1)^{k'+l'}}{N+1} \right], \quad (11b)$$

$$\tilde{\sigma}_{xy}^{k,l(c)} = \frac{r^2}{4} (\delta_{l',k'} + \delta_{l',k'-1}) \sum_m \frac{U_{4k'-2,m} U_{4l',m} \lambda_m}{1 + (\lambda_m r)^2}, \quad (11c)$$

$$\tilde{\sigma}_{xy}^{k,l(d)} = \delta_{k',l'} \sum_m U_{4k',m} U_{4l',m} \frac{2 + (\lambda_m r)^2}{4(1 + (\lambda_m r)^2)}. \quad (11d)$$

where $k' \equiv \lfloor \frac{k+1}{2} \rfloor_G$ and $l' \equiv \lfloor \frac{l+1}{2} \rfloor_G$. From these results, it is apparent that interlayer conductivity is finite only within nearest or second nearest layers (property ii). For the simplest example, the values of $\tilde{\sigma}_{xy}^{k,l}$ for three layer system obtained from the above formalism are $\tilde{\sigma}_{xy}^{1,1} = (2 + 3r^2 + r^4)/(4 + 8r^2)$, $\tilde{\sigma}_{xy}^{1,2} = r^2/(4 + 8r^2)$, $\tilde{\sigma}_{xy}^{2,2} = (2 + 2r^2)/(4 + 8r^2)$, $\tilde{\sigma}_{xy}^{1,3} = -r^4/(4 + 8r^2)$, with $\tilde{\sigma}_{xy}^{2,3} = \tilde{\sigma}_{xy}^{1,2}$ and $\tilde{\sigma}_{xy}^{3,3} = \tilde{\sigma}_{xy}^{1,1}$. In this case, $\sigma_{xy}^{1,3}$ becomes negative. By summing up all contributions, we obtain $\sum_{k,l} \tilde{\sigma}_{xy}^{k,l} = 3/2$ which consists of contributions from effective monolayer (1/2) and bilayer (1). For other N cases, these analytical results coincide with the general results summarized in Fig. 3(a) and (b).

—*Conclusion and discussion*— To conclude, we have studied the interlayer electronic transport properties of multilayer graphenes in a magnetic field for variety of stacking orders. The behaviour of the layer-resolved con-

ductivity depends strongly on the stacking structure. For AB stacking, various interesting properties, such as negative response, and suppression of the Hall conductivity, are identified. The breakdown of the quantization of the Hall conductivity indicates that interlayer conductivity has different features from those of the total response, and is not protected by topology.

Finally, we discuss the possibility of the experimental observation of the layer-resolved conductivities. Though it would be rather challenging to connect leads to particular layers, it is certainly easier to measure the layer-resolved conductivity between the top and the bottom layers. The fact that the longitudinal conductivity greatly changes according to the magnetic field (for example $\sigma_{xx}^{1,4}$ as shown in the inset of Fig. 3(c)) means that multilayer systems may be applied as switching device. We think that our work provides a comprehensive understanding of transport properties of multilayer graphene.

—*Acknowledgments*— We thank D.-H. Lee, M. Oshikawa, H. Shimada, and Y. Tada for discussions. M. N. acknowledges support from Global Center of Excellence Program “Nanoscience and Quantum Physics” of the Tokyo Institute of Technology and Grants-in-Aid No.23540362 by MEXT. B.D. was supported by the Hungarian Scientific Research Fund No. K72613, K73361, CNK80991, New Széchenyi Plan Nr. TÁMOP-4.2.1/B-09/1/KMR-2010-0002 and by the Bolyai program of the Hungarian Academy of Sciences is acknowledged.

-
- [1] K. S. Novoselov *et al.*, Science **306** 666 (2004).
 - [2] K. S. Novoselov *et al.*, Nature (London) **438** 197 (2005).
 - [3] Y. Zheng and T. Ando, Phys. Rev. B **65** 245420 (2002).
 - [4] V. P. Gusynin and S. G. Sharapov, Phys. Rev. Lett. **95** 146801 (2005).
 - [5] E. McCann and V. I. Fal’ko, Phys. Rev. Lett. **96** 086805 (2006).
 - [6] K. S. Novoselov *et al.*, Nature Phys. **2** 177 (2006).
 - [7] M. Nakamura, L. Hirasawa, and K. I. Imura, Phys. Rev. B **78** 033403 (2008).
 - [8] V. P. Gusynin and S. G. Sharapov, Phys. Rev. B **73** 245411 (2006).
 - [9] T. Ohta *et al.*, Phys. Rev. Lett. **98** 206802 (2007).
 - [10] W. Norimatsu and M. Kusunoki, Phys. Rev. B **81** 161410 (2010).
 - [11] Z. Liu *et al.*, Phys. Rev. Lett. **102** 015501 (2009).
 - [12] B. Partoens and F. M. Peeters, Phys. Rev. B **74** 075404 (2006).
 - [13] M. Koshino and T. Ando, Phys. Rev. B **76** 085425 (2007).
 - [14] M. Nakamura and L. Hirasawa, Phys. Rev. B **77** 045429 (2008).
 - [15] T. Maassen *et al.*, Phys. Rev. B **83** 115410 (2011).
 - [16] S. Yuan, H. DeRaedt, and M. I. Katsnelson, Phys. Rev. B **82** 235409 (2010).
 - [17] L. Zhang *et al.*, arXiv:1103.6023.
 - [18] M. Nakamura and L. Hirasawa, J. Phys.: Conf. Ser. **150** 022064 (2009).

- [19] A. Kumar *et al.*, arXiv:1104.1020.
- [20] H. Min *et al.*, Phys. Rev. B **83** 195117 (2011).
- [21] H. Min and A. H. MacDonald, Phys. Rev. B **77** 155416 (2008); Prog. Theor. Phys. Suppl. **176** 227 (2008).
- [22] M. Koshino and E. McCann, Phys. Rev. B **80** 165409 (2009).
- [23] M. Koshino and E. McCann, Phys. Rev. B **83** 165443 (2011).